

## Research Article

# Photodegradation of Malachite Green by Nanostructured $\text{Bi}_2\text{WO}_6$ Visible Light-Induced Photocatalyst

Yijie Chen, Yaqin Zhang, Chen Liu, Aimin Lu, and Weihua Zhang

College of Science, Nanjing Agricultural University, Nanjing 210095, China

Correspondence should be addressed to Weihua Zhang, whzhangnj@163.com

Received 14 August 2011; Accepted 6 September 2011

Academic Editor: Shifu Chen

Copyright © 2012 Yijie Chen et al. This is an open access article distributed under the Creative Commons Attribution License, which permits unrestricted use, distribution, and reproduction in any medium, provided the original work is properly cited.

$\text{Bi}_2\text{WO}_6$  photocatalyst was first utilized to degrade malachite green. The effects of the concentration of malachite green, the pH value, and the concentration of  $\text{Bi}_2\text{WO}_6$  on the photocatalytic efficiency were investigated. This study presents a strategy to eliminate highly toxic and persistent dyes such as malachite green.

## 1. Introduction

Malachite green is a kind of triphenylmethane dye which has been widely used in the production of ceramics, leather, textile industry, food coloring, cell coloring, and so on. Due to its high efficiency in disinfection, it has also been used in aquaculture industry to treat scratch on the fish bodies and defend against bacterial infections. Since 1990s, however, researchers found that malachite green and its reduced forms are highly toxic, persistent, carcinogenic, and mutagenic [1]. It will bring irretrievable damage to the environment if discharged into water body.

In recent years, much effort has been devoted to utilize photocatalysis to eliminate organic dyes in contaminated water [2–9].  $\text{TiO}_2$ -based nanomaterials are typical photocatalysts which have been extensively investigated, especially in the photodegradation of dyes [10–12].  $\text{TiO}_2$  possesses high activity in degrading pollutants under UV light irradiation and will not bring secondary pollution. However,  $\text{TiO}_2$  is only active under UV light irradiation, which is unfavorable for practical application [13–15]. Semiconductors of the Aurivillius oxides with general formula of  $\text{Bi}_2\text{A}_{n-1}\text{B}_n\text{O}_{3n+3}$  ( $A = \text{Ca}, \text{Sr}, \text{Ba}, \text{Pb}, \text{Na}, \text{K}$  and  $B = \text{Ti}, \text{Nb}, \text{Ta}, \text{Mo}, \text{W}, \text{Fe}$ ) have gained much attention due to their unique electronic structure and good stability [16]. Such oxides have become new types of highly effective photocatalysts.  $\text{Bi}_2\text{WO}_6$ , as a typical Aurivillius oxide ( $n = 1$ ), is attractive due to its narrow band gap, good stability, and excellent antioxidation ability. It has been reported that  $\text{Bi}_2\text{WO}_6$  could be used as a photocatalyst

to decompose water and degrade organic pollutants [17–20]. However, the investigated organic pollutants degraded by the photocatalysis of  $\text{Bi}_2\text{WO}_6$  are limited.

In this paper,  $\text{Bi}_2\text{WO}_6$  is firstly used as a photocatalyst to degrade a new kind of organic pollutant, malachite green. The effects of the concentration of malachite green, the pH value, and the concentration of photocatalyst on the degradation efficiency were studied. Under optimal condition, the degradation efficiency of malachite green is as high as ~100% only after 15 min of irradiation with  $\text{Bi}_2\text{WO}_6$  photocatalyst. These results reveal that  $\text{Bi}_2\text{WO}_6$  photocatalyst is a very perspective photocatalyst in wastewater remediation.

## 2. Experimental Section

All the reagents were of analytical purity and were used as received from Shanghai Chemical Company. In a typical process, aqueous solutions of  $\text{Bi}(\text{NO}_3)_3 \cdot 5\text{H}_2\text{O}$  and  $\text{Na}_2\text{WO}_4 \cdot 2\text{H}_2\text{O}$  in 2:1 molar ratio were mixed together, then the pH value of the final suspension was adjusted to about 7. The mixture was stirred for several hours at room temperature. Then the suspension was added into a 50 mL Teflon-lined autoclave up to 80% of the total volume. The suspension in the autoclave was heated at  $160^\circ\text{C}$  for 24 h under stirring. Subsequently, the autoclave was cooled to room temperature naturally. The products were collected by filtration and then were washed by deionized water and absolute ethanol until no anions were left in the solution as tested. The samples were then dried at  $80^\circ\text{C}$  for several hours.

The X-ray diffraction (XRD) patterns of the samples were measured on a D/MAX 2250V diffractometer (Rigaku, Japan) using monochromatized Cu K $\alpha$  ( $\lambda = 0.15418$  nm) radiation under 40 kV and 100 mA and scanning over the range of  $10^\circ \leq 2\theta \leq 80^\circ$ . The morphologies and microstructures of as-prepared samples were analyzed by transmission electron microscopy (TEM) (JEOL JEM-2100F, accelerating voltage 200 kV). The UV-vis diffuse reflectance spectra of the samples were recorded with a UV-vis spectrophotometer (Hitachi U-3010) using BaSO<sub>4</sub> as reference.

For photocatalysis test, typically aqueous Bi<sub>2</sub>WO<sub>6</sub> suspensions were prepared by adding certain amount of Bi<sub>2</sub>WO<sub>6</sub> into a 50 mL solution of malachite green with different concentration. The pH values of the suspensions were adjusted by adding KOH or HCl solution when necessary. Before illumination, the suspensions were magnetically stirred in dark to reach the adsorption/desorption equilibrium. A 500 W Xe lamp was used as the light source. The distance between the lamp and the suspension was kept at 20 cm. The experiments were processed at room temperature. At given time intervals, the suspension was sampled and centrifuged to remove the photocatalyst particles. For the photocatalytic degradation of malachite green under anoxic condition, N<sub>2</sub> bubbles were introduced into the reaction system for several hours to drive O<sub>2</sub> out, and then the reaction vessel was irradiated by Xe lamp. Malachite green exhibits the highest absorption at 616 nm, and the concentration of malachite green was monitored by the change of the absorption ( $A$ ) at 616 nm by a Shimadzu UV-1700 spectrophotometer in the photocatalytic reaction process. The degradation efficiency ( $\eta$ ) was described by the equation:  $\eta = (c_0 - c)/c_0 \times 100\% = (A_0 - A)/A_0 \times 100\%$  ( $c_0$  and  $c$  were the concentrations of malachite green at the beginning and after the photocatalytic reaction for certain time, while  $A_0$  and  $A$  were the absorption intensities at the beginning and after photocatalytic reaction for certain time).

### 3. Results and Discussions

The phase and composition of the products, which were prepared at neutral pH value and the temperature of 160°C for 24 hours, were investigated by using XRD measurement. Figure 1 shows the XRD pattern of the Bi<sub>2</sub>WO<sub>6</sub> sample. Obviously, the Bi<sub>2</sub>WO<sub>6</sub> sample exhibits high-intensity and narrow-diffraction peaks in the XRD pattern, which is due to the well crystallization. All the diffraction peaks can be indexed to orthorhombic Bi<sub>2</sub>WO<sub>6</sub> according to the JCPDS card no. 39-0256. After refinement, the crystal lattice parameter of Bi<sub>2</sub>WO<sub>6</sub> was calculated to be as follows:  $a = 5.456$  Å,  $b = 16.445$  Å, and  $c = 5.444$  Å.

As shown in Figure 2, the diffuse reflectance spectrum of as-prepared Bi<sub>2</sub>WO<sub>6</sub> indicates it absorbs visible light with wavelength shorter than 470 nm. The morphology and microstructure of the Bi<sub>2</sub>WO<sub>6</sub> samples were revealed by TEM images (Figures 3(a) and 3(b)). The panoramic view shown in Figure 3(a) demonstrates that the as-prepared product is composed of homogeneous nanoplates. Close observation revealed by high-magnification TEM image (Figure 3(b)) shows that most of these nanosized Bi<sub>2</sub>WO<sub>6</sub> are

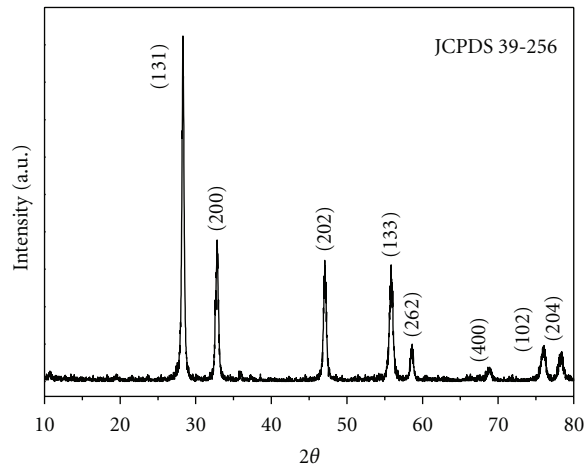


FIGURE 1: The XRD pattern of Bi<sub>2</sub>WO<sub>6</sub> sample prepared by hydrothermal method.

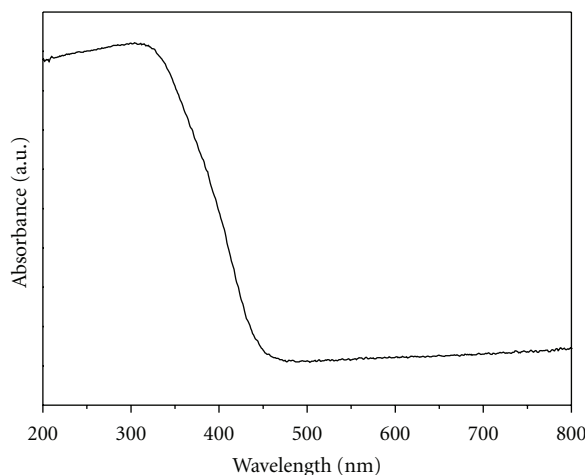


FIGURE 2: Diffuse reflectance spectrum of as-prepared Bi<sub>2</sub>WO<sub>6</sub> sample.

nanoplatelike. In addition, the shape and the size can also be observed clearly, which is platelike with size of about 200 nm.

The absorption spectrum of malachite green was shown in Figure 4(a). As demonstrated, the highest absorption appeared at 616 nm which was used to monitor the concentration of malachite green. The effect of the initial concentration of malachite green on the photocatalytic degradation rate was first investigated. The concentration of Bi<sub>2</sub>WO<sub>6</sub> was kept at 1 g·L<sup>-1</sup>, and the time of irradiation was 75 min. The malachite green solutions with the initial concentrations of 5 mg·L<sup>-1</sup>, 10 mg·L<sup>-1</sup>, 15 mg·L<sup>-1</sup>, and 20 mg·L<sup>-1</sup> were prepared, respectively. As shown in Figure 4(b), the degradation efficiency of malachite green decreased when the initial concentration increased, and the trend was accelerated when the concentration became higher. This phenomenon could be explained as follows. Malachite green molecule is photosensitive. More photons would be absorbed when the concentration increased, leading to relatively low light transmittance. Thus, the depth of light

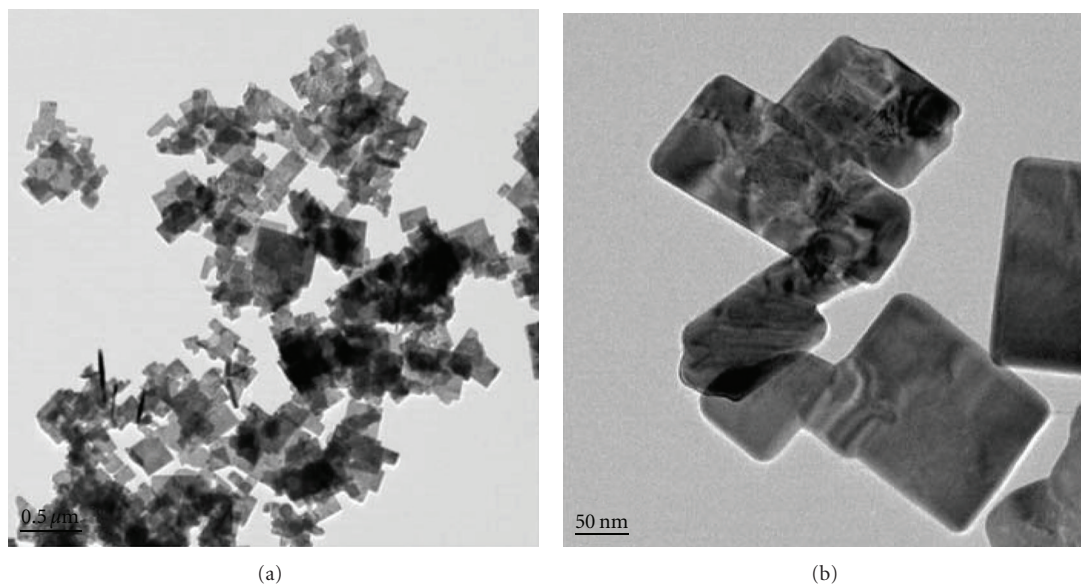


FIGURE 3: The TEM images of as-synthesized  $\text{Bi}_2\text{WO}_6$  nanoplates: (a) low magnification, (b) high magnification.

penetration decreased, and the photocatalytic activity of  $\text{Bi}_2\text{WO}_6$  was inhibited. Less  $\text{Bi}_2\text{WO}_6$  would be activated, and the degradation efficiency of dye decreases accordingly [21].

The effect of pH value on the degradation efficiency of malachite green in the range that the solution possesses a stable color of blue was further investigated. The pH value of the original solution of malachite green is 5.3. Diluted hydrochloride acid solution or potassium hydroxide solution was used to tune the pH value when necessary. The initial concentration of malachite green solution and the concentrations of the photocatalyst were kept at  $10 \text{ mg}\cdot\text{L}^{-1}$  and  $1 \text{ g}\cdot\text{L}^{-1}$ , respectively. Various solutions of different pH values of 2, 4, 5.3, and 8 were prepared. After 30 min of photocatalytic irradiation, degradation efficiencies were compared. As illustrated in Figure 5, the degradation efficiency of malachite green solution decreased when the pH value of the reaction solution increased. The degradation efficiency of the malachite green solution was 98.9% when pH value was 2, while the degradation efficiency was 30.63% when pH value was 8. The observed dependence may be ascribed to the pH value effect on the photocatalyst. The oxidation of organic compounds involving the diffusion of organic compound to the particle surface so as to form a complex firstly, followed by the exchange of electrons with the reactive surface of oxides has been reported [22]. Since malachite green has an anionic configuration, the adsorption is favored in acidic solution. The prevailing pH value of the solution affects the mode and extent of adsorption of malachite green on the  $\text{Bi}_2\text{WO}_6$  surface and thus, indirectly, affects the photodegradation efficiency of malachite green. On the other hand, in the catalytic process,  $\text{H}^+$  can enhance the surface acidity of  $\text{Bi}_2\text{WO}_6$  and make the malachite-green molecules more prone to interact with  $\text{Bi}_2\text{WO}_6$ . These effects lead to the observed increase in the degradation efficiency with decreased pH value.

The cost of photocatalyst was the primary factor contributing to the chemical costs of photocatalytic treatment. It is important to minimize the required amount of photocatalyst. Thus, the investigation of  $\text{Bi}_2\text{WO}_6$  concentrations on the degradation of malachite green dye was conducted, which is shown in Figure 6. The initial concentration and the pH value of malachite green solution are kept at  $10 \text{ mg}\cdot\text{L}^{-1}$  and 2, respectively. The concentrations of  $\text{Bi}_2\text{WO}_6$  are set at  $0.2 \text{ g}\cdot\text{L}^{-1}$ ,  $0.6 \text{ g}\cdot\text{L}^{-1}$ ,  $1.0 \text{ g}\cdot\text{L}^{-1}$ ,  $1.4 \text{ g}\cdot\text{L}^{-1}$ , and  $1.8 \text{ g}\cdot\text{L}^{-1}$ , respectively. After 10 min of photocatalytic degradation, the degradation efficiencies were compared. In Figure 6, the photocatalytic degradation performance is relatively undesirable. The degradation efficiency of malachite green solution increased with the increase of the concentration of  $\text{Bi}_2\text{WO}_6$  until the concentration of  $\text{Bi}_2\text{WO}_6$  reached to  $1.0 \text{ g}\cdot\text{L}^{-1}$ , while corresponding degradation efficiency was 87.04%. However, the degradation efficiency changed little when the concentration of  $\text{Bi}_2\text{WO}_6$  was more than  $1.0 \text{ g}\cdot\text{L}^{-1}$ . This can be explained on the basis that optimum photocatalyst loading is dependent on initial solute concentration. If the concentration of photocatalyst was increased, the total active surface was increased correspondingly, and as a result, the enhanced photocatalytic performance was obtained. However, the increased concentration of photocatalyst would have no effect on promoting the degradation efficiency after a maximum photocatalyst concentration was imposed. This may be ascribed to the increased aggregation of photocatalyst at high concentration. Therefore, the optimal concentration of  $\text{Bi}_2\text{WO}_6$  in current case is  $1.0 \text{ g}\cdot\text{L}^{-1}$ .

According to above experiments, the optimal conditions for photocatalytic degradation of malachite green are as follows: the initial concentration of malachite green, pH value, and the concentration of  $\text{Bi}_2\text{WO}_6$  are  $10 \text{ mg}\cdot\text{L}^{-1}$ , 2, and  $1.0 \text{ g}\cdot\text{L}^{-1}$ , respectively. Figure 7 shows the evolution of the degradation of malachite green with irradiation time. It is

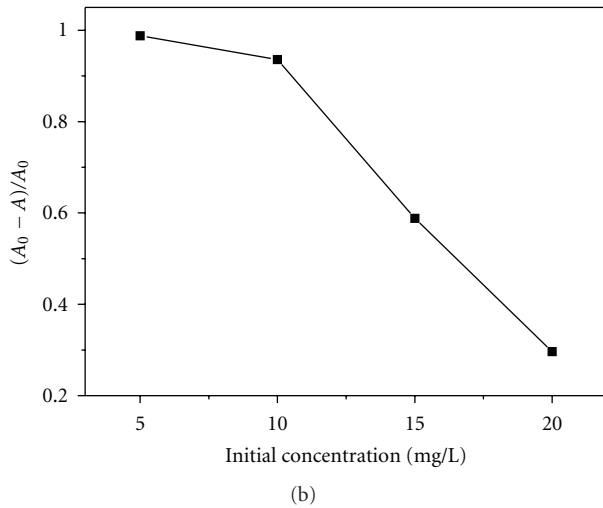
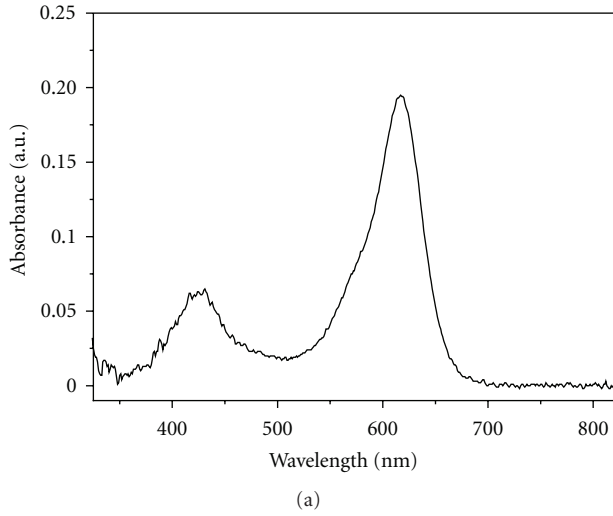


FIGURE 4: (a) The absorption spectrum of malachite green. (b) The effect of the initial concentration of malachite green on the degradation efficiency.

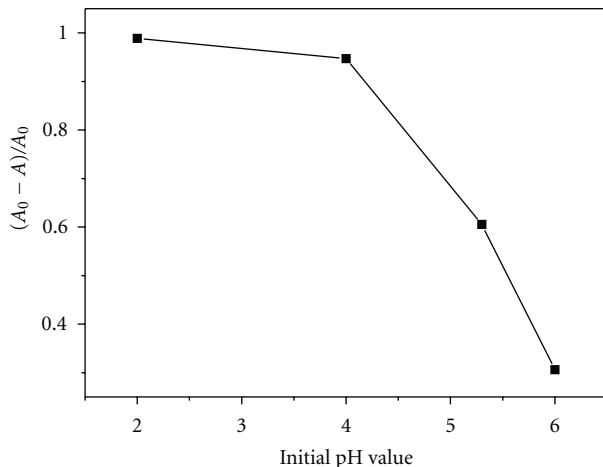


FIGURE 5: The effect of initial pH value on the degradation efficiency.

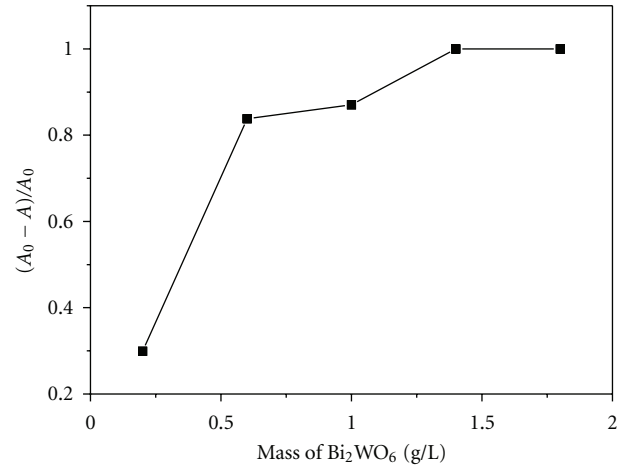


FIGURE 6: The effect of the concentration of photocatalyst on the degradation efficiency.

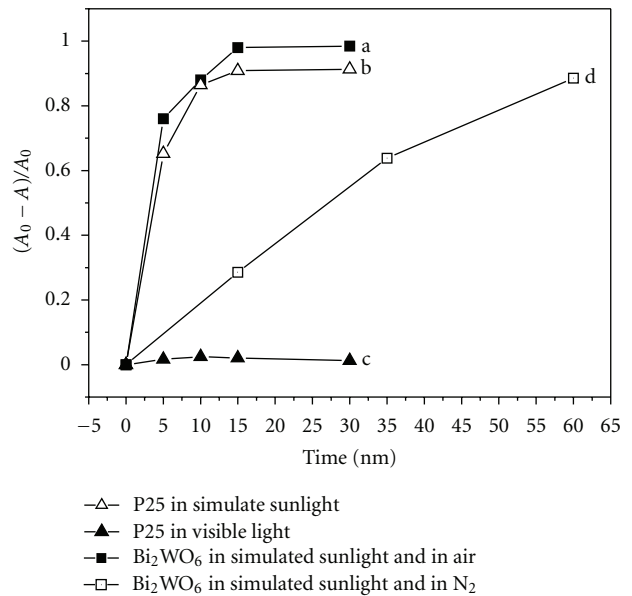


FIGURE 7: The photocatalytic degradation of malachite green time under optimal conditions (the initial concentration of malachite green, initial pH value, and the concentration of photocatalyst are 10 mg·L<sup>-1</sup>, 2, and 1.0 g·L<sup>-1</sup>, resp.): (a) Bi<sub>2</sub>WO<sub>6</sub> under Xe lamp (as indicated by black square; (b) reference P25 under Xe lamp (as indicated by white triangle, simulated sunlight); (c) reference P25 under visible light (as indicated by black triangle); (d) Bi<sub>2</sub>WO<sub>6</sub> under visible light and anoxic condition.

revealed that the degradation of malachite green solution was fast during the initial 5 min of photocatalytic reaction. Then it decreased gradually. According to earlier reports, [23–25] the relation between the rate of photocatalytic degradation and the concentration of photocatalyst can be expressed by the Langmuir-Hinshelwood equation:  $r = -dc/dt = kKc/(1 + Kc)$ . When the concentration of substrate is low ( $Kc \ll 1$ ), the Langmuir-Hinshelwood equation can be

expressed as  $r = -dc/dt = kKc$ . Thus, the rate of photocatalytic degradation is proportional to the concentration of photocatalyst. For the degradation of malachite green solution, the concentration of malachite green gradually decreased during the photocatalytic degradation. As a result, the photocatalytic degradation is relatively fast during the initial 5 min. For the malachite green solution with the initial concentration of  $10 \text{ mg}\cdot\text{L}^{-1}$  and pH value of 2, the color of the solution hardly changed in the dark without any photocatalyst. For the same malachite green solution, the degradation efficiency with  $\text{Bi}_2\text{WO}_6$  photocatalyst in the dark for 90 min is only 13.6%, which can be attributed to the adsorption of malachite green on  $\text{Bi}_2\text{WO}_6$  photocatalyst. And the degradation efficiency without photocatalyst is 13.56% after 15 min under light irradiation, which is due to the photolysis of malachite green. These comparison experiments revealed that the decrease of malachite green is mainly caused by the photocatalytic degradation.

For comparison, a typical commercial  $\text{TiO}_2$ , P25, was selected as the reference. Under simulated solar light, it exhibited comparable activity as that of the  $\text{Bi}_2\text{WO}_6$  (Figure (7b)). However, as indicated by Figure (7c), under visible light irradiation P25 exhibited poor photocatalytic activities in the photodegradation of malachite green because, it can only be activated by UV light. In order to check if oxygen molecules affected the degradation process, the photocatalytic degradation of malachite green was carried out under  $\text{N}_2$ -saturated conditions. The result shown in Figure (7d) indicates that under the anoxic condition, the photodegraded rate was largely suppressed.

#### 4. Conclusion

In conclusion, a visible light-induced  $\text{Bi}_2\text{WO}_6$  nanoplate photocatalyst was hydrothermally synthesized at neutral pH values and at a temperature of  $160^\circ\text{C}$  for 24 h. The obvious degradation of malachite green was only observed with  $\text{Bi}_2\text{WO}_6$  photocatalyst under light irradiation. The photocatalytic performance of the  $\text{Bi}_2\text{WO}_6$  sample was found greatly influenced by the concentration of photocatalyst, the concentration of malachite green, and the pH value of the reaction system. The optimum concentration of photocatalyst was  $1.0 \text{ g}\cdot\text{L}^{-1}$  for the degradation of  $10 \text{ mg}\cdot\text{L}^{-1}$  malachite green solution with the pH value of 2. In addition, the relation between the rate of photocatalytic degradation and the concentration of malachite green can be described by the pseudo-first-order kinetics, rationalizing in terms of the Langmuir-Hinshelwood model.

#### Acknowledgment

The authors acknowledge the financial support from the Key Laboratory of Pesticide Chemistry of Jiangsu Province (NYXKT201005).

#### References

[1] K. V. K. Rao, "Inhibition of DNA synthesis in primary rat hepatocyte cultures by malachite green: a new liver tumor

- promoter," *Toxicology Letters*, vol. 81, no. 2-3, pp. 107–113, 1995.
- [2] A. Fujishima, T. N. Rao, and D. A. Tryk, "Titanium dioxide photocatalysis," *Journal of Photochemistry and Photobiology C*, vol. 1, no. 1, pp. 1–21, 2000.
- [3] M. R. Hoffmann, S. T. Martin, W. Choi, and D. W. Bahnemann, "Environmental applications of semiconductor photocatalysis," *Chemical Reviews*, vol. 95, no. 1, pp. 69–96, 1995.
- [4] M. A. Fox and M. T. Dulay, "Heterogeneous photocatalysis," *Chemical Reviews*, vol. 93, no. 1, pp. 341–357, 1993.
- [5] J. C. Zhao, T. X. Wu, K. Q. Wu, K. Oikawa, H. Hidaka, and N. Serpone, "Photoassisted degradation of dye pollutants. 3. Degradation of the cationic dye rhodamine B in aqueous anionic surfactant/ $\text{TiO}_2$  dispersions under visible light irradiation: evidence for the need of substrate adsorption on  $\text{TiO}_2$  particles," *Environmental Science and Technology*, vol. 32, no. 16, pp. 2394–2400, 1998.
- [6] W. Choi and S. Kim, "Kinetics and mechanisms of photocatalytic degradation of  $(\text{CH}_3)_n\text{NH}_{4-n}^+$  ( $0 \leq n \leq 4$ ) in  $\text{TiO}_2$  suspension: the role of OH radicals," *Environmental Science and Technology*, vol. 36, no. 9, pp. 2019–2025, 2002.
- [7] C. C. Wong and W. Chu, "The hydrogen peroxide-assisted photocatalytic degradation of alachlor in  $\text{TiO}_2$  suspensions," *Environmental Science and Technology*, vol. 37, no. 10, pp. 2310–2316, 2003.
- [8] Y. M. Xu and C. H. Langford, "UV- or visible-light-induced degradation of X3B on  $\text{TiO}_2$  nanoparticles: the influence of adsorption," *Langmuir*, vol. 17, no. 3, pp. 897–902, 2001.
- [9] W. Ho, J. C. Yu, J. Lin, and P. Li, "Preparation and photocatalytic behavior of  $\text{MoS}_2$  and  $\text{WS}_2$  nanocluster sensitized  $\text{TiO}_2$ ," *Langmuir*, vol. 20, no. 14, pp. 5865–5869, 2004.
- [10] J. H. Carey, J. Lawrence, and H. M. Tosine, "Photodechlorination of PCB's in the presence of titanium dioxide in aqueous suspensions," *Bulletin of Environmental Contamination and Toxicology*, vol. 16, no. 6, pp. 697–701, 1976.
- [11] S. N. Frank and A. J. Bard, "Heterogeneous photocatalytic oxidation of cyanide and sulfite in aqueous solutions at semiconductor powders," *Journal of Physical Chemistry*, vol. 81, no. 15, pp. 1484–1488, 1977.
- [12] L. Q. Jing, X. J. Sun, J. Shang et al., "Review of surface photovoltage spectra of nano-sized semiconductor and its applications in heterogeneous photocatalysis," *Solar Energy Materials and Solar Cells*, vol. 79, no. 2, pp. 133–151, 2003.
- [13] R. Asahi, T. Morikawa, T. Ohwaki, K. Aoki, and Y. Taga, "Visible-light photocatalysis in nitrogen-doped titanium oxides," *Science*, vol. 293, no. 5528, pp. 269–271, 2001.
- [14] A. L. Linsebigler, G. Lu, and J. T. Yates Jr., "Photocatalysis on  $\text{TiO}_2$  surfaces: principles, mechanisms, and selected results," *Chemical Reviews*, vol. 95, no. 3, pp. 735–758, 1995.
- [15] J. Yu, L. Zhang, Z. Zheng, and J. Zhao, "Synthesis and characterization of phosphated mesoporous titanium dioxide with high photocatalytic activity," *Chemistry of Materials*, vol. 15, no. 11, pp. 2280–2286, 2003.
- [16] L. S. Zhang, W. Z. Wang, L. Zhou, and H. L. Xu, " $\text{Bi}_2\text{WO}_6$  Nano- And microstructures: shape control and associated visible-light-driven photocatalytic activities," *Small*, vol. 3, no. 9, pp. 1618–1625, 2007.
- [17] A. Kudo and S. Hiji, " $\text{H}_2$  or  $\text{O}_2$  evolution from aqueous solutions on layered oxide photocatalysts consisting of  $\text{Bi}^{3+}$  with  $6s^2$  configuration and  $d^0$  transition metal ions," *Chemistry Letters*, vol. 28, no. 10, pp. 1103–1104, 1999.

- [18] J. W. Tang, Z. G. Zou, and J. H. Ye, "Photocatalytic decomposition of organic contaminants by  $\text{Bi}_2\text{WO}_6$  under visible light irradiation," *Catalysis Letters*, vol. 92, no. 1-2, pp. 53–56, 2004.
- [19] M. Shang, W. Z. Wang, and H. L. Xu, "New  $\text{Bi}_2\text{WO}_6$  nanocages with high visible-light-driven photocatalytic activities prepared in refluxing EG," *Crystal Growth and Design*, vol. 9, no. 2, pp. 991–996, 2009.
- [20] M. Shang, W. Z. Wang, S. M. Sun, L. Zhou, and L. Zhang, " $\text{Bi}_2\text{WO}_6$  nanocrystals with high photocatalytic activities under visible light," *Journal of Physical Chemistry C*, vol. 112, no. 28, pp. 10407–10411, 2008.
- [21] C. C. Chen, C. S. Lu, Y. C. Chung, and J. L. Jan, "UV light induced photodegradation of malachite green on  $\text{TiO}_2$  nanoparticles," *Journal of Hazardous Materials*, vol. 141, no. 3, pp. 520–528, 2007.
- [22] A. T. Stone, "Reductive dissolution of manganese(III/IV) oxides by substituted phenols," *Environmental Science and Technology*, vol. 21, no. 10, pp. 979–988, 1987.
- [23] M. Saquib and M. Muneer, " $\text{TiO}_2$ /mediated photocatalytic degradation of a triphenylmethane dye (gentian violet), in aqueous suspensions," *Dyes and Pigments*, vol. 56, no. 1, pp. 37–49, 2003.
- [24] F. Sayilkan, M. Asiltürk, P. Tatar, N. Kiraz, E. Arpaç, and H. Sayilkan, "Photocatalytic performance of Sn-doped  $\text{TiO}_2$  nanostructured mono and double layer thin films for Malachite Green dye degradation under UV and vis-lights," *Journal of Hazardous Materials*, vol. 144, no. 1-2, pp. 140–146, 2007.
- [25] F. Sayilkan, M. Asiltürk, P. Tatar et al., "Photocatalytic performance of Sn-doped  $\text{TiO}_2$  nanostructured thin films for photocatalytic degradation of malachite green dye under UV and VIS-lights," *Materials Research Bulletin*, vol. 43, no. 1, pp. 127–134, 2008.



**Hindawi**

Submit your manuscripts at  
<http://www.hindawi.com>

